Biointerface Research in Applied Chemistry
Open-Access Journal (ISSN: 2069-5837)

Article
Volume 13, Issue 1, 2023, 54
https://doi.org/10.33263/BRIAC131.054

New Organic Dyes with Low Bandgap Based on Heterocyclic Compounds for Dye-sensitized Solar Cells Applications

Marzouk Raftani [1,*], **Tayeb Abram** [2], **Ahmed Azaid** [1], **Rchid Kacimi** [2], **Mohammed Naciri Bennani** [4], **Mohammed Bouachrine** [1,3,*]

[1] Molecular Chemistry and Natural Substances Laboratory, Faculty of Sciences, University Moulay Ismail, Meknes, Morocco
[2] MEM (LASMAR) ESTM, University Moulay Ismail, Meknes, Morocco
[3] EST Khenifra, Sultan Moulay Sliman University, Beni mellal, Morocco
[4] Laboratory of Chemistry and Biology Applied to the Environment, Faculty of Sciences, My Ismail University, Morocco
* Correspondence: m.bouachrine@est-umi.ac.ma (M.B.); m.raftani@edu.umi.ac.ma (M.R.);
Scopus Author ID 8983993500

Received: 16.11.2021; Accepted: 15.12.2021; Published: 30.01.2022

Abstract: In this paper, a theoretical study has been carried out. This study concerns four organic dyes with structure D–π–A on the base of triphenylamine; we choose thiophene and thieno [3, 4-b] pyrazine group as a donor and the group cyanoacrylic acid as an acceptor bridged by four conjugated spacers consisting of phenyl, pyrrole, thiophene, and furan. Our studied dyes' ground state geometric and electronic properties are calculated after optimization in their fundamental states with DFT / B3LYP / 6−311G (d, p). Using this method, EHOMO, ELUMO, bandgap energy, λmax, chemical reactivity indices, dipole moment, the Voc, molecular electrostatic potential (MEP), the LHE, the free injection energy (ΔGinj), the regeneration energy (ΔGreg), and the total reorganization energy (λtot) for all these dyes have been calculated and discussed. The optical properties such as Etr, the maximum wavelength (λmax), and the corresponding oscillator strengths have been carried out by the TD−DFT method at CAM–B3LYP/6–311G (d, p). The calculated results for all these dyes indicate that all these latters can be considered favorable candidates for an efficient DSSC sensitizer.

Keywords: organic dyes; DSSC; photovoltaic parameters; TD–DFT–CAM/B3LYP; Thiophene.

1. Introduction

Solar energy becomes the most competitive alternative to substitute fossil fuels to satisfy the increasing energy demand [1]. Photovoltaic refers to directly converting light harvested to electrical energy employing a semiconductor material [2]. Therefore, the development of new photovoltaic devices becomes indispensable. Different new photovoltaic systems have been developed and are going through the process to be commercialized [3]. Thus, enormous researchers focus their efforts to develop solar cell elements, principally for solar cells DSSC type [4]. The dye-sensitized solar cells (DSSC), The DSSC, since they have been first reported by O'Regan and Grätzel *et al*. in 1991 [5], have been pulled tremendous attention thanks to low cost, lightweight nature, and high performance of photovoltaic to develop flexible photovoltaic devices [2-5]. The DSSC devices consist of four units: photoanode [6], cathode [7], electrolyte, and sensitizer [8]. The photoanode consists of a nanocrystalline semiconductor film such as TiO$_2$ on a glass substrate [9]. The sensitizer is an important element in dye-sensitized solar cells that plays a crucial role in harvesting light and injecting the electrons [10]. Electrolyte contains a redox couple as I^-/I_3^-, closed by a counter electrode (often platinum) [11]. Presently, most organic dyes own the D-π-A structure, aiming to facilitate intramolecular charge transfer (ICT) from the donor (D) to the acceptor (A) across the π-bridge [12].

Besides this structure (D-π-A), another configurations like D-D-π-A [12], D-A-π-A [13], D-π-A-A [14], (D-π-A)$_2$ [15] have also been developed and drawn more attention [16]. As mentioned above, the structure (D-π-A) is the most prevalent [16,17]. This is because of its electronic mobility facilitation, and therefore optimizes the efficacy of the dyes such that they are utilized in Grätzel cells [4,18]. Therefore, the quality of a DSSC cell is intimately linked to the specific light-sensitive dye utilized in the cell [19]. So, to get a better rendering of DSSCs, the following characteristics must be used [20]: (i) it must have the most suitable conjugation betwixt donor (D) and acceptor (A) across the π-linker; (ii) it is necessary to possess a wide and great absorption band which can cover almost every the visible spectral region and near-infrared one (NIR); (iii) a proper redox and oxidation capacities of the dye examined to ease regeneration; (iv), and for accelerating charge transfer of such a dye to TiO$_2$ [21], robust electronic conjunction amidst such dye and CB of TiO$_2$ must be [20]. To design a dye as a sensitizer for devices DSSCs, it is necessary to investigate some of their electronic and optoelectronic properties. The HOMO should be under the redox couple's energy level so that the dye can be regenerated efficiently (iodide/triiodide I^-/I^-_3) [22]. On the opposite side, to facilitate injection of the electron within the anode, the LUMO energy level should be on top of the CB of the TiO2 [23]. Further, for allowing effective harvesting of the light, the two following arguments must be that the dye should also absorb into visible or near-infrared (NIR) areas and great molar extinction coefficient [23].

Several organic dyes as a donating group of electrons like triphenylamine [24], carbazole [25], indoline [26] ,and phenothiazine [27] are synthesized and designed aiming to facilitate high DSSC performances [2]. The most often used groups betwixt the donor unit and the acceptor one as π-linkers are phenyls, thiophene, and their derivatives (furan, pyrrole...); who are accountable for charge transfer [28]. On the other side, some electron acceptors moieties, such as benzotriazole [29], diketopyrrolopyrrole [30], and benzothiadiazole [31], have been used aiming to model a novel and highly effective generation of dyes [13,32]. The typical organic sensitizer contains a D-π-A structure [33]. As mentioned above, several functional groups are used aiming to arrange and sensitize the D-π-A structure organic sensitizer [34]. The organic dye triphenylamine is one of these functional groups that have been widely studied [35]. This group functional presents a good electron-donating property, a non-planar molecular structure that prohibits aggregation. These properties prove to be an excellent electron donor [36] and a good candidate for DSSC. The cyanoacrylic acid (the 2-cyanoprop-2-enoic acid) is used in the majority of the D-π-A organic dyes as an acceptor moiety thanks to the attendance of the cyano group (which is an electron-withdrawing) close of the carboxylic acid group that enhances the spectral response across the intramolecular charge transfer in addition to its capacity of injecting electrons [1].

In this paper, the DFT computations are achieved on a series from conjugated dyes to predict their optimized structure and electronic properties like the HOMO, LUMO, and bandgap energy. The studied dyes contain a triphenylamine, thiophene, and thieno [3, 4-b] pyrazine fragment which is considered as donor unit, cyanoacrylic acid is an electron acceptor unit, different π-linkers join the two units D and A as example phenyl, thiophene, pyrrole and furan [37].

The objective of this work is to study the influence of π-bridges on the electronic and photovoltaic parameters of the four organic dyes named D_A-Phe (D_1), D_A-Pyr (D_2), D_A-Thi (D_3), and D_A-Fur (D_4). Several important parameters can affect dye performances like energy levels HOMO and LUMO, energy bandgap, dipole moment, E_{00}, which means the lowest excitation energies, Light-Harvesting Efficiency (LHE), energy corresponding to open-circuit voltage noted (V_{oc}), the free energy of injection (ΔG^{inj}) and the regeneration energy (ΔG^{reg}) have been conducted. The electrochemical, photovoltaic, and absorption parameters of the studied compounds (dyes) are systematically investigated using the DFT and TD-DFT quantum methods. The chemical structure of the studied dyes is shown in figure 1.

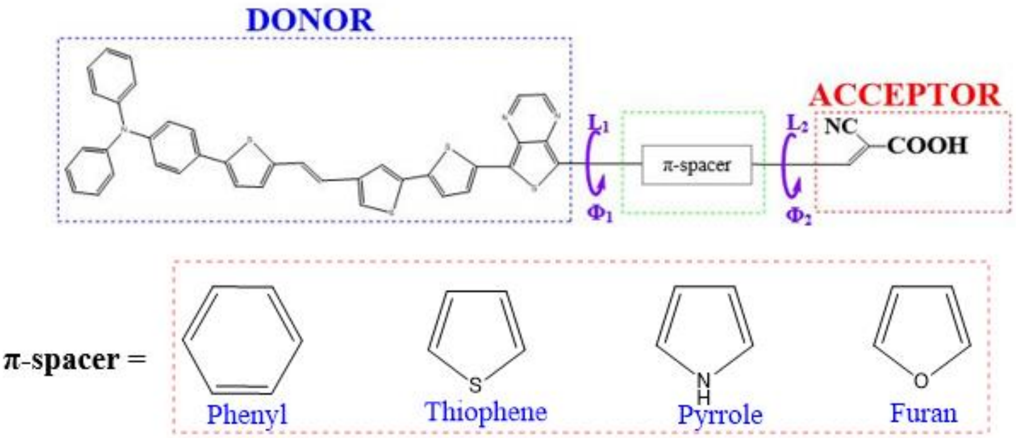

Figure 1. Chemical structures of the investigated compounds.

2. Materials and Methods

2.1. Computational details.

The DFT using the functional (B3LYP) [38] at the 6-311G (d) basis set [39] have been utilized for optimizing the geometries in their fundamental state and also theoretically computing of the electronic, optic, and photovoltaic parameters for the designed dyes having a D-π-A structure to possible use in DSSCs. Gaussian 09 software package [40] has been used to achieve the theoretical calculations. The time-dependent quantum method TD-DFT [41] with the functional CAM-B3LYP [42] is applied to calculate optical parameters and the absorption spectra. The HOMO, LUMO, bandgap, wavelength λ_{max}, and oscillator strength (f) have been carried out using quantum calculations.

Various parameters can determine the performance of a DSSC, one the most generally used parameter is power conversion efficiency (PCE) noted (η), this latter parameter depends on several other parameters such as short-circuit current density (Jsc), Fill Factor (FF), open-circuit voltage (V_{oc}) and the incident solar power (P_{in}) [43]. The power conversion efficiency can be expressed by the following formula:

$$\eta = FF\frac{V_{oc}\,J_{sc}}{P_{inc}} \quad (1)$$

The V_{oc} parameter (open-circuit voltage) can be estimated as [44]:

$$V_{oc} = E_{LUMO} - E_{CB} \quad (2)$$

Where E_{LUMO} is the energy level, LUMO of the dye and (E_{CB}) is considered as the energy of the conduction band (CB) of the semiconductor (commonly TiO_2) (E_{CB} = - 4.0 eV) [45].

In DSSCs, the J_{sc} is generally estimated as follows [46]:

$$J_{SC} = \int_{\lambda}^{0} LHE(\lambda)\phi_{Inj}\eta_{Coll} d\lambda \quad (3)$$

Here, the parameter LHE (λ) is linked to the oscillator strength (f) at a designated maximum wavelength, Φ_{inject} is considered as electron injection within the conductance band of the TiO_2, and $\eta_{collect}$ parameter signifies charge collection efficiency. To know the theoretical relation betwixt the J_{sc} and PCE, several parameters like Φ_{inj}, LHE, and reorganization energy (λ_{tot}) are examined. The LHE can be determined as [47].

$$LHE(\lambda) = 1 - 10^{-f} \quad (4)$$

For studied dyes, the injection driving force ΔG^{inj} has been calculated by the expression [48]:

$$\Delta G^{inj} = E^{dye*} - E_{CB} \quad (5)$$

E^{dye*} denotes the oxidation potential of the dye in an excited state, and it can be determined as follows [49]:

$$E^{dye*} = E^{dye} - E_{00} \quad (6)$$

E^{dye} signifies the oxidation potential of the dye in the neutral state ($E_{dye} = - E_{HOMO}$), while E_{00} is considered as the vertical transition energy which corresponds to λ_{max} [50].

The regeneration driving force (ΔG^{reg}) is expressed as follows [51]:

$\Delta G^{reg} = E^{dye} - E_{Redox}^{Electrolyte}$ (7)Where $E_{Redox}^{Electrolyte}$ is denoted as redox potential of the electrolyte I^-/I^-_3 (−4.80 eV) [52].

The positive and negative states of dyes are optimized through the DFT method, aiming to determine the reorganization energies (λ_{tot}) [53]. It is noted that to have a high value of Jsc, a low value of reorganization energy (λ_{total}) is needed; that could be determined by adding the hole reorganization energy to the electron one [12] as follows [54]:

$$\lambda_i = \left|E_0^{\mp} - E_{\mp}^{\mp}\right| - \left|E_{\pm}^{0} - E_0\right| \quad (8)$$

Noted that $E_0^{\pm}$ designate the energy of cation (anion), which is determined in the neutral state from their optimized structure, $E_{\pm}^{\pm}$ indicate the energy of cation (anion) determined in the cationic (anionic) state from the optimized structure, $E_{\pm}^{0}$ is the calculated energy at the cationic (anionic) state of the neutral molecule. Finally, E_0 designates the computed energy at the fundamental state of the neutral molecule. Moreover, the cations and anions concerning the creation of "electron holes". The two parameters of the dyes, such ionization potential (IP) and the electronic affinity (EA) have been carried out as follows:

$$IP = E(M^+) - E(M_0) \quad (9)$$

$$EA = E(M_0) - E(M^-) \quad (10)$$

The E_0 (M), E (M^+), and E (M^-) designate the total energy of the neutral, positive (cationic) respectively, and negative (anionic) state.

Several global reactivity parameters have been introduced in the chemical literature [55] example the chemical potential (μ), electronegativity (χ) [56] and hardness (η) [57,58]. Knowing the values HOMO and LUMO energy levels for such a compound, these various parameters can be calculated via the following formulas [59,60]:

$$- \mu = (E_{HOMO} + E_{LUMO})/2; \quad (11)$$

$$- \eta = (E_{LUMO} - E_{HOMO})/2; \quad (12)$$

$$- \chi = -(E_{HOMO} + E_{LUMO})/2; \quad (13)$$

3. Results and Discussion

3.1. Molecular geometry.

Figure 2 display the chemical structures of the investigated molecules. Using DFT/B3LYP/6-311G (d, p), all molecular geometries have been carried out [61]. The data in figure 2 exhibits that all organic dyes possess nearly planar conformations [62]. In D-π-A type compounds, the π-conjugated group exists as a linker for intermolecular charge transfer (ICT), the bonds between D and π-spacer (L_1), between and A and π-spacer (L_2) furnish an account of the interrelationships among themselves [63]. To gain from intramolecular charge transfer in the D-π-A type compounds, a short link length of the bridge is needed. The critical bonds lengths (L_1 and L_2) and the dihedrals angles (Φ_1 and Φ_2) of investigated molecules in their ground state and excited one are collected in table 1. As illustrated in figure 1, the dihedral angle between the donor and π-spacer is named Φ_1 while and these betwixt the acceptor and π-spacer is Φ_2.

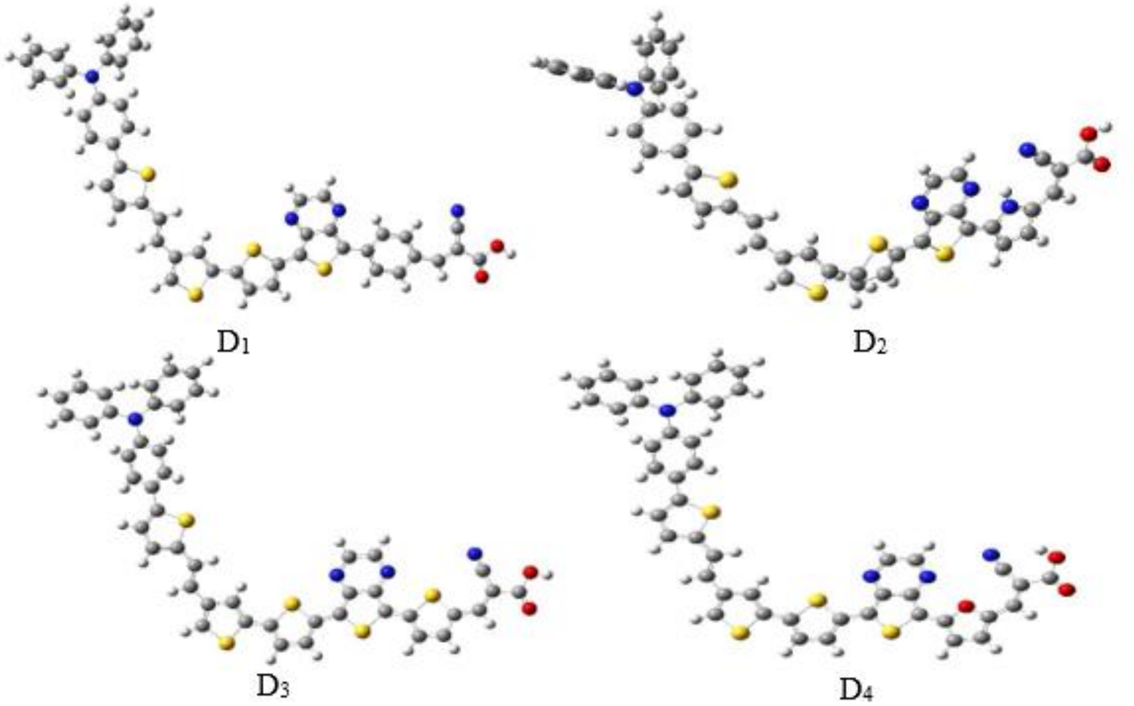

Figure 2. The obtained optimized structures of the investigated organic dyes by DFT−B3LYP/6−311G (d, p).

Table 1. The obtained geometrical data L_i (Å) and Φ_i (°) for the investigated dyes by B3LYP/6−311G (d, p).

Dyes	**L_1**		**L_2**		**Φ_1**		**Φ_2**	
	S_0	**S_1**	**S_0**	**S_1**	**S_0**	**S_1**	**S_0**	**S_1**
D_1	1.43	1.45	1.42	1.45	176.40	168.18	179.42	179.64
D_2	1.43	1.42	1.41	1.42	179.88	179.95	179.86	179.97
D_3	1.43	1.43	1.42	1.43	179.74	179.95	179.93	179.88
D_4	1.43	1.42	1.41	1.42	179.03	179.06	179.84	179.97

It is remarked from the results exhibited in the table above that the bond lengths values L_1 for all dyes in their ground state (S_0) are 1.43 Å; that is to say, the bond lengths are between C–C bonds which facilitates the ICT process of the dyes. For all the dyes, L_2 change significantly, and their values are 1.41 Å for D_2 and D_4 and are 1.42 Å for D_1 and D_3 [64]. It implies that the interplay midst acceptor moiety and π-spacer are barely influenced by the interactions D-π [65]. From Table 1, it can be observed that Φ_2 in all compounds in their fundamental state is similar (179°); whereas Φ_1 values of all molecules are similar (179°), except for D_1 (168.18°). These obtained values indicate that all molecules have planar geometry except for the dihedral angle betwixt the donor and π-spacer for D_1 dye, which is somewhat twisted likely because of the existence of steric effects between the two groups donor and acceptor [66,67]. It is believed that this planar molecular structure ought to ameliorate the transfer of electrons from the D to A across the π-spacer unit for these dyes [68]. Therefore, the insertion of phenyl moiety as π-spacer is unfavorable to the molecular planarity and the effect of conjugation [69]. Finally, for these studied compounds in the excited state (S1) the getting values of Li and Φ_i are almost analogous compared to those in the ground state (S_0).

3.2. Molecular orbitals.

Generally, the choice of the appropriate donor group and acceptor one is required to ameliorate the light-gathering capacity of DSSCs [62]. So, in dyes with the D-π-A type, the electron-donating ability (D) can affect the electrochemical properties [61]. Regarding D-π-A type organic dyes, a high value of the energy level HOMO is provided by a stronger electron-donating group. In contrast, the great electron-accepting group supplies a low energy level E_{LUMO}. To provide a profound vision into the outbuilding of the electronic properties on the structure of molecules [70], it is helpful to theoretically determine the energy levels HOMO and LUMO for any molecule, seeing that this knowledge informs whether the proposed dyes meet the basic requirements for a photosensitizer from DSSC [71]. The analysis of the HOMO and LUMO energies levels and the relevant energy gap of our studied dyes are given in figure 3. The FMO diagram is presented in figure 4.

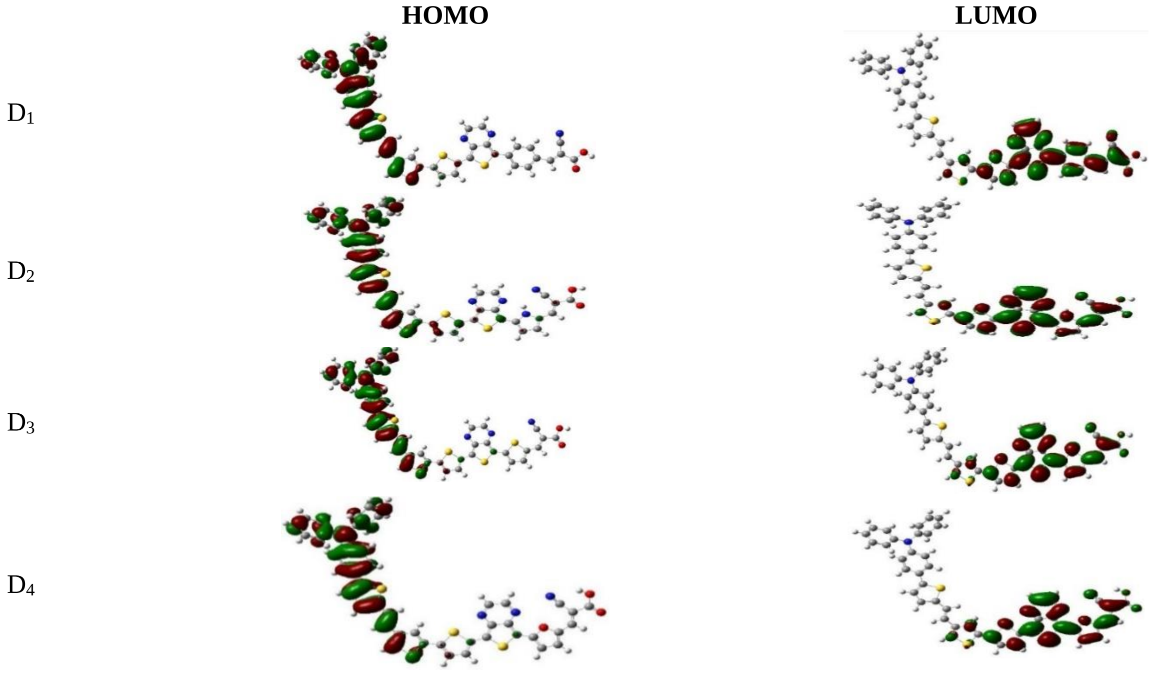

Figure 3. The contour plots of frontier orbitals (HOMO and LUMO) for all studied dyes.

Figure 3 indicates that the electrons of HOMO are mainly distributed on the donor moiety, raft whereas a high electron density is exhibited on the π-spacer moieties as well as the acceptor one for any dyes. This means that there is an electron delocalization [70]. On the first hand, the HOMO possesses a π-bonding character in the sub-fragments as well as a π-antibonding one betwixt successive sub-fragments [72]; on the other hand, the LUMO's exhibit a π-antibonding character in the sub-fragments as well as a π-bonding character betwixt the sub-fragments [73]. Generally, the molecule containing a more density of HOMO ought to own a great ability to provide electrons [74], while the one occupied by more density of LUMO is more comfortable acquiring the electrons [75]. HOMO's electron density transfers to the LUMO one during photoexcitation of the sensitizer producing a great transition of the ICT.

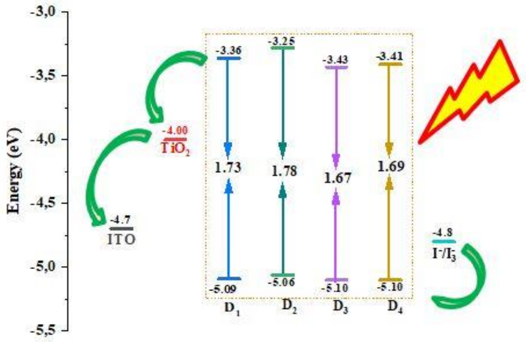

Figure 4. Energy levels diagram of all dyes.

The HOMO, LUMO, and bandgap are indispensable implements for injecting dye's electrons into the semiconductor's conduction band. Hence, the energies of HOMO, LUMO, and bandgap of the considered molecules are calculated by the B3LYP/ 6−311G (d, p) and presented in table 2.

From the results above, the obtained values of energies levels occupied as well as unoccupied (HOMO/LUMO) for D_1, D_2, D_3, and D_4 are respectively -5.09/-3.36 eV, -5.06/-3.26 eV, -5.10/-3.43 eV and -5.10/-3.41 eV, the corresponding energies bandgap for these dyes are 1.73 eV, 1.78 eV, 1.67eV and 1.69 eV, respectively. These obtained values exhibit that our designed molecules are suitable candidates for a photosensitizer because of their HOMO energy levels situated below the redox couple level I^-/I^-_3 (-4.8 eV) [22], and the values of the energy level LUMO are located up of the conduction band of the semiconductor (-4.0 eV) [23]. Furthermore, the obtained values of the bandgap are between 1.67 and 1.78 eV. This implicates that the studied dyes can be used in DSSCs [2]. It can be remarked that the E_{gap} decreases as follows: $D_2 > D_1 > D_4 > D_3$. Subsequently, the E_{gap} of these dyes is weak. This is probably influenced by π-conjugated donor units and the π-bridge ones leading to a rise in the charge transfer betwixt the donor group and the acceptor one.

Table 2. The obtained values of the electronic as well as the chemical indices parameters of the four dyes.

Compounds	**E_{HOMO} (eV)**	**E_{LUMO} (eV)**	**E_g (eV)**	**η (eV)**	**μ (eV)**	**χ (eV)**	**ρ (D)**
D_1	-5.09	-3.36	1.73	0.87	-4.23	4.23	7.18
D_2	-5.06	-3.28	1.78	0.89	-4.17	4.17	4.87
D_3	-5.10	-3.43	1.67	0.84	-4.27	4.27	6.80
D_4	-5.10	-3.41	1.69	0.85	-4.26	4.26	8.84
TiO_2	−	-4.00					

3.3. Quantum chemical parameters.

To better understand the reactivity in molecular systems in their ground state [76], electronic chemical potential (μ), global hardness (η), and electronegativity (χ) are estimated using the DFT method. The chemical potential (μ) may represent an electron's propensity to leave an equilibrium system [77]; Whereas chemical hardness (a) is known to be a marker for measuring stability and reactivity that are related to intramolecular charge transfer resistance (ICT) [74]. Electronegativity (χ) is the opposite value of the chemical potential and can be defined as the system's electron-donor property [66]. These quantum parameters are determined from the energy levels of HOMO and LUMO.

According to the obtained results figured in Table 2, the chemical potentials of the four molecules are superior to the value of TiO_2. This means that electrons can readily skip to the TiO_2 from these dyes, showing that these molecules behave as optimal donors' groups of electrons for solar cells applications. It should be noted that as the chemical hardness decreases, the conversion efficiency increases [78]. The four dyes' chemical hardness ascending order is as follows: $D_3 < D_4 < D_1 < D_2$. The electronegativity values of all dyes are lower than those of TiO_2 one, indicating that TiO_2 is capable of pulling the electrons of these compounds. The electronegativity values of all dyes are 4.23 eV, 4.17 eV, 4.27 eV, and 4.26 eV, respectively. The potential chemical values are greater than TiO_2 for the investigated dyes. This signifies that electrons readily jump from the Di dyes to the TiO_2 [70]. Finally, from table 2, the computed values of dipole moment (ρ) parameter for D1, D2, D3, and D4 dyes are 7.18 eV, 4.87 eV, 6.80 eV, and 8.84 eV. The obtained dipole moment values for D_1, D_3, and D_4 are comparatively higher than those for D_2, indicating that the latter are more reactive [66].

3.4. Electrostatic potential (ESP).

We conducted calculations for the electrostatic potentials of the investigated dyes with DFT-B3LYP/6-311G. (d, p). The MEP is a plot showing the electrostatic potential, charted onto the constant electron density surface [79], that focuses on predicting the physicochemical properties such as the reactive sites for the attack of the electrophilic nucleophilic [80]. MEP offers a 3D vision system for recognizing the electrostatic impact of a molecule [81]. Furthermore, it provides a tool for analyzing the related polarity of the compounds [82]. The ESP maps of the designated dyes are illustrated in figure 5.

ESP values are displayed in different colours. The blue region indicates electron-poor regions, whereas the red region indicates an electron-rich field [70]. The map color code falls between the two values -5.628 e^{-2} (deepest red) and 5.628 e^{-2} (deepest blue) for D_1, −0.128 e^{0} (deepest red) and 0.128 e^{0} (deepest blue) for D_2, -5.855 e^{-2} (deepest red) and 5.855 e^{-2} (deepest blue) for D_3, -6.020 e^{-2} (deepest red) and 6.020 e^{-2} (deepest blue) for D_4.

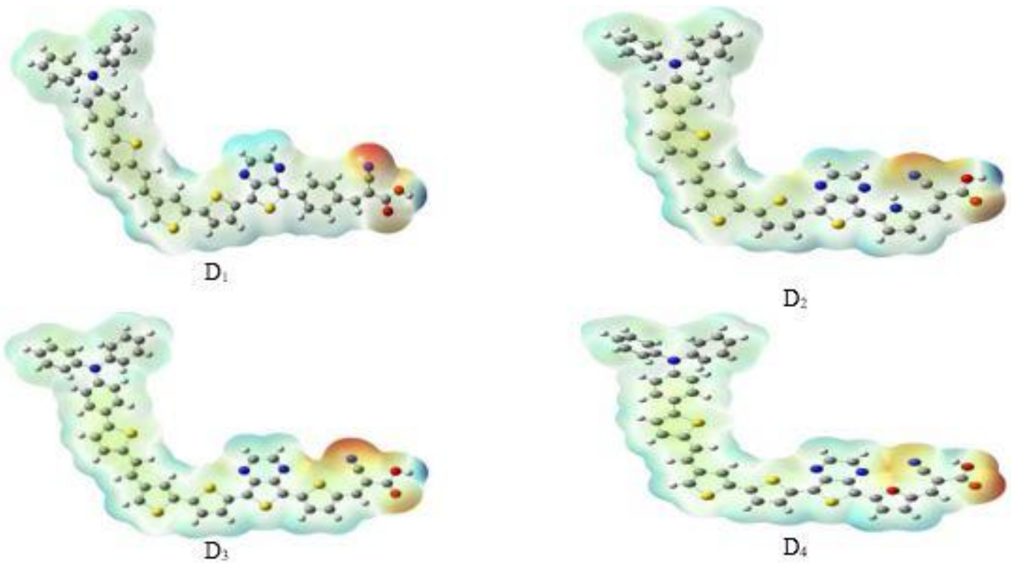

Figure 5. Molecular ESP Mapping of the Di dyes.

3.5. Photovoltaic performances.

For the donor and acceptor elements, their energy levels HOMO and LUMO influence whether an effective charge transfer will occur between the donor D_i and acceptor (TiO_2) [70]. The study results show that all dyes' energy level LUMO is far superior to that of the CB for TiO_2 (-4.0 eV) [23]. This indicates that HOMO and LUMO energies levels can be influenced by photo-excited electron transfer from these investigated dyes. Hence, a study of the impact of varying the π-spacer of these dyes on the electronic properties has been achieved.

Therefore, D_4 presents a great HOMO value (-5.10 eV), designating that the furan unit presents powerful electron-donor conduct relative to other π-spacers [20]. It has been shown that the furan unit shows an important oxidation potential, which makes it more effective as a dye sensitizer [83]. Lastly, it can be noticed that the energy levels values LUMO of all investigated compounds are insignificantly influenced by replacing π-spacer groups. This exhibits that this parameter is linked to the acceptor group (cyanoacrylic acid).

Using equations in the Computational detailssection, different parameters like f, LHE, E_{ex}, E^{dye*}, ΔG^{inj}, ΔG^{reg}, λ_{total}, and V_{oc} for the four dyes have been studied and listed in table 3. Using quantum methods DFT and TD-DFT, the optical parameters such as f, LHE, and E_{ex} have been computed.

Table 3. Calculated energy values of IP, EA, LHE, V_{oc}, ΔG^{inj}, ΔG^{reg}, reorganization energies (λ_e), (λ_e) and (λ_{tot}).

Dyes	**IP**	**EA**	λ_e	λ_h	λ_{tot}	E_{00}	E^{dyes}	E^{dyes*}	ΔG^{inj}	ΔG^{reg}	V_{oc}
D_1	5.930	2.340	0.276	0.248	0.524	2.220	5.090	2.870	-1.130	0.290	0.640
D_2	5.890	2.180	0.285	0.212	0.497	2.100	5.060	2.960	-1.040	0.260	0.720
D_3	5.920	2.400	0.285	0.219	0.504	2.090	5.100	3.010	-0.990	0.300	0.570
D_4	5.930	2.370	0.289	0.221	0.510	2.160	5.100	2.940	-1.060	0.300	0.590

Evaluating the performances of an organic dye depends on an important parameter that is the LHE. Here, all the resulting values of the LHE parameter for the four dyes are betwixt 0.89 and 0.93. Since the LHE values of these dyes are in a close range, these dyes give approximately the same photocurrent response.

A feeble negative value of G^{inj} and a small value of G^{reg} are needed the acceptable sensitizers. Moreover, lower G^{reg} is sufficient to prevent the recombination process and minimize dye degradation [51]. From Table 3, all studied dyes have a negative value of ΔG^{inj}; this can be explained by the excited state occupying the upper conduction band of Titanium dioxide. This reveals that the electron injection process from dye to TiO_2 is spontaneous. It can be observed that D_3 has a greater ΔG^{inj} value (maximal value – 0.99 eV), while D_1 has the smallest one (minimal value – 1.13 eV). This study indicates that D1 has the greatest driving force of electron injection in all designed dyes, whereas D_3 has the least.

On the other hand, the regeneration energy (ΔR^{reg}) for any dyes is positive, indicating that the sensitizer fundamental state situates under the electrolyte redox couple, which is why electron recombination is suppressed [84,85]. For designed dyes, the ΔGreg value of D_3 (3.00 eV) is the greater value than others, suggesting that D_3 regenerates more rapidly than other dyes [66]. Consequently, D_1 electron injection could be quicker than other dyes, and on the other hand, the D_3 dye regeneration rate could be quicker than the other designed dyes [86].

Besides the short-circuit current density J_{sc}, the PCE (η) could also be affected by another parameter, that is, the energy corresponding to the open-circuit voltage (V_{oc}). Based on Eq. (2), the computed V_{oc} values for any dyes range between 0.57 V and 0.72 V (see Table 3). The estimated values theoretically of V_{oc} decrease as follows: $D_2 > D_1 > D_4 > D_3$. It can be noticed that D_2 has a larger V_{oc} value than other dyes, while D_3 has the tiniest one. These results advise that photoexcited electrons in the dyes might jump into the conduction band of TiO_2, which helps increase the effectiveness of photoconversion in photovoltaic systems.

In addition, the reorganization energy (λ_{tot}) is a necessary factor in deciding the equipoise properties for hole and electron transport, whereas petty λtot is capable of accelerating charge carrier transport speeds, and the converse is true for larger reorganization energy [87]. Therefore, to analyze the correlation betwixt the J_{sc} and the electronic structure, the calculating of the λ_{tot} is also necessary [65]. As cited above in the Computational details part, the λ_{tot} consists of the hole (λ_h) and electron (λ_e) energies. Thus, the small λ_{tot} could improve the J_{sc}. The findings listed in table 3 indicate that computed λ_{tot} of designed dyes are between 0.497 eV to 0.524 eV and decrease as follows $D_2 < D_3 < D_4 < D_1$. It is shown that the dye D_2 has the smallest λ_{tot} energy, whereas D_1 possesses the largest one.

Moreover, The appropriate and balanced transport of both injected electrons and hole is critical in determining the performance of electronic devices [88]. Thus, the energy barrier for the electron and hole injection in a given dye can be determined by computing the DFT of the ionization potential and electron affinity [65]. The major challenge that the application in the LEDs is the need to achieve an n-type conjugated molecule to boost electron injection and transport. Also, It is a challenge for organic electronic devices to boost hole injection/transport when a p-type conjugated molecule at low ionization potential is used [89]. It is shown from Table 3 that the energies needed for holes' injection in these dyes are: 5.930, 5.890, 5.812, 5.920, and 5.930 eV, respectively. They are all low. This is coherent with the analysis of HOMO energy [90].

3.6. Optical properties.

It is necessary to study the absorption spectrum, which is a crucial property of a DSSC dye [2]. It is important to measure the absorption spectrum of the studied compounds for use in DSSCs to decide whether a material is acceptable for photovoltaic applications [75]. Indeed, wide and large visible absorption properties are necessary to have a good photovoltaic compound. The optical properties like E_{Tr}, f, and λ_{abs} of the studied dyes have been investigated using CAM–B3LYP/6–311G (d, p) [91]. These parameters are displayed in table 4, and absorption spectra are presented in figure 6.

Table 4. Absorption spectra for all dyes obtained by TD−DFT/CAM−B3LYP/6−311G (d, p).

Compounds	**λ_{abs} (nm)**	**E_{Tr} (eV)**	**f**	**LHE**	**MO/Character**
D_1	557.70	2.22	1.13	0.93	H-1 --> L (75%)
	399.87	3.10	0.02	0.05	H --> L (72%)
	368.21	3.37	1.77	0.98	H --> L+2 (52%)
D_2	590.14	2.10	0.94	0.89	H-1 --> L (65%)
	400.44	3.10	0.07	0.15	H --> L (53%)
	376.38	3.29	0.64	0.77	H-1 --> L+1 (49%)
D_3	593.59	2.09	1.13	0.93	H-1 --> L (74%)
	413.90	3.00	0.02	0.05	H --> L (68%)
	379.51	3.27	0.47	0.66	H-1 --> L+1 (64%)
D_4	574.64	2.16	1.10	0.92	H-1 --> L (77%)
	411.25	3.01	0.02	0.05	H --> L (71%)
	379.04	3.27	0.22	0.40	H-1 --> L+1 (71%)

The absorption spectra arising from the excited state (S_1) are assigned to the HOMO-1→ LUMO transition for the four dyes. These absorption bands were allocated to ICT betwixt electron donor and the acceptor [63]. The greatest absorption peak of these dyes is localized around 593 nm for D_3. The obtained values of wavelength λ_{max} for the considered dyes decrease as follows: D_3 (593.59 nm) > D_2 (590.14 nm) > D_4 (574.64 nm) > D_1 (557.70 nm).

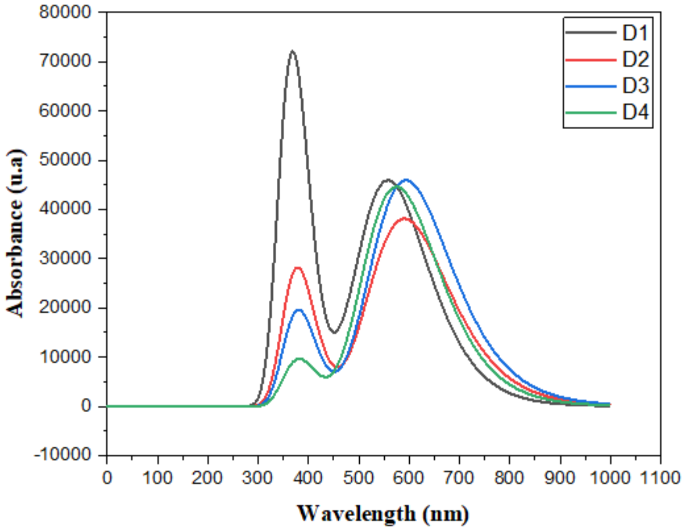

Figure 6. Absorption spectra obtained with TD−DFT CAM−B3LYP/6−311G (d, p).

The dyes give a bathochromic absorption when crossing from D_3 (559.59 nm) to D_1 (557.70 nm) which may be attached to the increment of the π-conjugation during replacing the phenyl ring by pyrrole or thiophene ring in the π-spacer [20]. From figure 6, the absorption spectra exhibit two peaks: one is a huge peak situated betwixt 500 and 900 nm, and another one is located among the 300–450 nm wavelength region. This means these molecules possess a single band within the visible region (where λ_{max}> 400 nm). This is probably because of the rise in conjugation length through the π-spacer part [92]. As a result, it can be deduced that these studied dyes may be useful as donor compounds in photovoltaic devices.

4. Conclusions

In this work, several geometric, electronic, photovoltaic, and optical properties of four D_1-D_4 dyes have been theoretically investigated using quantum chemical methods DFT and TD-DFT. Modifying the chemical structures of investigated materials may considerably adjust and ameliorate both electronic and optical properties. Their electronic properties are investigated for our conjugated dyes based on triphenylamine, thiophene, and thieno [3, 4-b] pyrazine as the donor and various π-spacer groups the mentioned method above. It is found that changing the acceptor moiety ameliorates the photovoltaic properties of the investigated dyes by destabilizing and stabilizing the HOMO and LUMO levels, respectively. This leads to decreasing the E_g value, growing the geometrical planarity, increasing the absorption wavelength λ_{max}, and improving the injection of electrons and dye regeneration.

Computations show that the obtained values of the bandgap are from 1.67 to 1.78 eV. This implicates that the investigated dyes possess the ability to be used in DSSCs. The energies levels LUMO of these dyes are located above the CB of the TiO_2, proposing that transferring a photoexcited electron from Di toward TiO2 can be advantageous in photovoltaic materials. Calculated values of V_{oc} for these dyes vary between 0.57 V and 0.72 V, meaning that these are enough to be an effective injection of electrons possibly. The obtained values of wavelength λ_{max} for the investigated dyes D_1, D_2, D_3, and D_4 are 557.70 nm, 590.14 nm, 593.59 nm, and 574.64 nm, respectively.

In summary, the most suitable dye that can be applied in photovoltaic devices like donor of electrons in solar cell DSSCs type is a small bandgap, broad wavelengths, relevant FMO levels, great values of LHE and ΔG^{inj}, as well as the lowest λ_{tot}. Therefore, our studied dyes D_i are suitable to perform this function

Funding

This research received no external funding.

Acknowledgments

This research has no acknowledgment.

Conflicts of Interest

The authors declare no conflict of interest.

References

1. Duerto, I.; Colom, E.; Andrés-Castán, J.M.; Franco, S.; Garín, J.; Orduna, J.; Villacampa, B.; Blesa, M.J. DSSCs based on aniline derivatives functionalized with a tert-butyldimethylsilyl group and the effect of the π-spacer. *Dyes and Pigments* **2018**, *148*, 61-71, https://doi.org/10.1016/j.dyepig.2017.07.063.
2. ElKhattabi, S.; Hachi, M.; Fitri, A.; Benjelloun, A.T.; Benzakour, M.; McHarfi, M.; Bouachrine, M. Theoretical study of the effects of modifying the structures of organic dyes based on N,N-alkylamine on their efficiencies as DSSC sensitizers. *Journal of Molecular Modeling* **2019**, *25*, 1-9, https://doi.org/10.1007/s00894-018-3888-0.
3. Ahmad, S.; Yum, J.H.; Xianxi, Z.; Grätzel, M.; Butt, H.J.; Nazeeruddin, M.K. Dye-sensitized solar cells based on poly (3,4-ethylenedioxythiophene) counter electrode derived from ionic liquids. *Journal of Materials Chemistry* **2010**, *20*, 1654-1658, https://doi.org/10.1039/b920210b.
4. dos Santos, G.C.; Oliveira, E.F.; Lavarda, F.C.; da Silva-Filho, L.C. Designing new quinoline-based organic photosensitizers for dye-sensitized solar cells (DSSC): a theoretical investigation. *Journal of Molecular Modeling* **2019**, *25*, https://doi.org/10.1007/s00894-019-3958-y.
5. ’O’Regan, B.; Gratzel, M. A Low-Cost, High-Efficiency Solar-Cell Based on Dye-Sensitized Colloidal TiO2 Films. *Nature* **1991**, *353*, 737-740, https://doi.org/10.1038/353737a0.
6. Park, N.G.; van de Lagemaat, J.; Frank, A.J. Comparison of Dye-Sensitized Rutile- and Anatase-Based TiO2 Solar Cells. *The Journal of Physical Chemistry B* **2000**, *104*, 8989-8994, https://doi.org/10.1021/jp994365l.
7. Hauch, A.; Georg, A. Diffusion in the electrolyte and charge-transfer reaction at the platinum electrode in dye-sensitized solar cells. *Electrochimica Acta* **2001**, *46*, 3457-3466, https://doi.org/10.1016/S0013-4686(01)00540-0.
8. Robertson, N. Optimizing Dyes for Dye-Sensitized Solar Cells. *Angew. Chem. Int. Ed* **2006**, *45*, 2338-2345, https://doi.org/10.1002/anie.200503083.
9. Birel, Ö.; Nadeem, S.; Duman, H. Porphyrin-Based Dye-Sensitized Solar Cells (DSSCs): a Review. *Journal of Fluorescence* **2017**, *27*, 1075-1085, https://doi.org/10.1007/s10895-017-2041-2.
10. Wu, H.; Huang, Z.; Hua, T.; Liao, C.; Meier, H.; Tang, H.; Wang, L.; Cao, D. Metal-free organic dyes with di(1-benzothieno)[3,2-b:2′,3′-d]pyrrole as a donor for efficient dye-sensitized solar cells: Effect of mono- and bi-anchors on photovoltaic performance. *Dyes and Pigments* **2019**, *165*, 103-111, https://doi.org/10.1016/j.dyepig.2019.02.003.
11. Das, P.; Ganguly, S.; Maity, P.P.; Bose, M.; Mondal, S.; Dhara, S.; Das, A.K.; Banerjee, S.; Das, N.C. Waste chimney oil to nanolights: A low cost chemosensor for tracer metal detection in practical field and its polymer composite for multidimensional activity. *Journal of Photochemistry and Photobiology B: Biology* **2018**, *180*, 56-67, https://doi.org/10.1016/j.jphotobiol.2018.01.019.
12. Bourass, M.; Touimi Benjelloun, A.; Benzakour, M.; McHarfi, M.; Hamidi, M.; Bouzzine, S.M.; Serein-Spirau, F.; Jarrosson, T.; Sotiropoulos, J.-M.; Bouachrine, M. The optoelectronic properties of new dyes based on thienopyrazine. *Comptes Rendus Chimie* **2017**, *20*, 461-466, https://doi.org/10.1016/j.crci.2016.12.004.
13. Wu, Y.; Zhu, W. Organic sensitizers from D–π–A to D–A–π–A: Effect of the internal electron-withdrawing units on molecular absorption, energy levels and photovoltaic performances. *Chemical Society Reviews* **2013**, *42*, 2039-2058, https://doi.org/10.1039/c2cs35346f.

14. Lin, L.Y.; Tsai, C.H.; Lin, F.; Huang, T.W.; Chou, S.H.; Wu, C.C.; Wong, K.T. 2,1,3-Benzothiadiazole-containing donor-acceptor-acceptor dyes for dye-sensitized solar cells. *Tetrahedron* **2012**, *68*, 7509-7516, https://doi.org/10.1016/j.tet.2012.05.052.
15. Seo, K.D.; You, B.S.; Choi, I.T.; Ju, M.J.; You, M.; Kang, H.S.; Kim, H.K. Dual-channel anchorable organic dyes with well-defined structures for highly efficient dye-sensitized solar cells. *Journal of Materials Chemistry A* **2013**, *1*, 9947-9953, https://doi.org/10.1039/c3ta11832k.
16. Wu, H.; Liao, C.; Tang, H.; Wang, L.; Meier, H.; Cao, D. Metal-free organic dyes with di(1-benzothieno)[3,2-b:2′,3′-d]pyrrole as an auxiliary donor for efficient dye-sensitized solar cells: Effect of the molecular engineering on the photovoltaic performance. *Dyes and Pigments* **2019**, *171*, https://doi.org/10.1016/j.dyepig.2019.107676.
17. Fitri, A.; Benjelloun, A.T.; Benzakour, M.; McHarfi, M.; Hamidi, M.; Bouachrine, M. Theoretical studies of the master factors influencing the efficiency of thiazolothiazole-based organic sensitizers for DSSC. *Journal of Materials and Environmental Science* **2016**, *7*, 835-844.
18. Hagfeldt, A.; Boschloo, G.; Sun, L.; Kloo, L.; Pettersson, H. Dye-Sensitized Solar Cells. *Chem. Rev* **2010**, *110*, 6595-6663, https://doi.org/10.1021/cr900356p.
19. Shah, S.A.A.; Sayyad, M.H.; Wahab, F.; Khan, K.A.; Munawar, M.A.; Elbohy, H.; Qiao, Q. Synthesis, modeling and photovoltaic properties of a benzothiadiazole based molecule for dye-sensitized solar cells. *Journal of Materials Science: Materials in Electronics* **2016**, *27*, 4501-4507, https://doi.org/10.1007/s10854-016-4324-9.
20. Sadki, H.; Bourass, M.; Bennani, M.N.; Bouachrine, M. New organic materials based on D–π–A structure for application in dye-sensitized solar cells. *Research on Chemical Intermediates* **2018**, *44*, 6071-6085, https://doi.org/10.1007/s11164-018-3476-z.
21. Preat, J. Photoinduced energy-transfer and electron-transfer processes in dye-sensitized solar cells: TDDFT insights for triphenylamine dyes. *Journal of Physical Chemistry C* **2010**, *114*, 16716-16725, https://doi.org/10.1021/jp1050035.
22. Nazeeruddin, M.K. Michael Graetzel Festschrift, a tribute for his 60th Birthday. *Coordination Chemistry Reviews* **2004**, *248*, 1161-1164, https://doi.org/10.1016/j.ccr.2004.06.011.
23. El Khattabi, S.; Fitri, A.; Benjelloun, A.T.; Benzakour, M.; McHarfi, M.; Hamidi, M.; Bouachrine, M. Theoretical investigation of electronic, optical and photovoltaic properties of alkylamine-based organic dyes as sensitizers for application in DSSCs. *Journal of Materials and Environmental Science* **2018**, *9*, 841-853, https://doi.org/10.1007/s00894-018-3888-0.
24. Lee, D.H.; Lee, M.J.; Song, H.M.; Song, B.J.; Seo, K.D.; Pastore, M.; Anselmi, C.; Fantacci, S.; De Angelis, F.; Nazeeruddin, M.K.; Gräetzel, M.; Kim, H.K. Organic dyes incorporating low-band-gap chromophores based on π-extended benzothiadiazole for dye-sensitized solar cells. *Dyes and Pigments* **2011**, *91*, 192-198, https://doi.org/10.1016/j.dyepig.2011.03.015.
25. Wang, Z.S.; Koumura, N.; Cui, Y.; Takahashi, M.; Sekiguchi, H.; Mori, A.; Kubo, T.; Furube, A.; Hara, K. Hexylthiophene-functionalized carbazole dyes for efficient molecular photovoltaics: Tuning of solar-cell performance by structural modification. *Chemistry of Materials* **2008**, *20*, 3993-4003, https://doi.org/10.1021/cm8003276.
26. Wu, Y.; Zhang, X.; Li, W.; Wang, Z.S.; Tian, H.; Zhu, W. Hexylthiophene-featured D-A-π-a structural indoline chromophores for coadsorbent-free and panchromatic dye-sensitized solar cells. *Advanced Energy Materials* **2012**, *2*, 149-156, https://doi.org/10.1002/aenm.201100341.
27. Tian, H.; Yang, X.; Chen, R.; Pan, Y.; Li, L.; Hagfeldt, A.; Sun, L. Phenothiazine derivatives for efficient organic dye-sensitized solar cells. *Chemical Communications* **2007**, 3741-3743, https://doi.org/10.1039/b707485a.
28. Liu, B.; Wang, R.; Mi, W.; Li, X.; Yu, H. Novel branched coumarin dyes for dye-sensitized solar cells: Significant improvement in photovoltaic performance by simple structure modification. *Journal of Materials Chemistry* **2012**, *22*, 15379-15387, https://doi.org/10.1039/c2jm32333h.
29. Cui, Y.; Wu, Y.; Lu, X.; Zhang, X.; Zhou, G.; Miapeh, F.B.; Zhu, W.; Wang, Z.S. Incorporating benzotriazole moiety to construct D-A-π-A organic sensitizers for solar cells: Significant enhancement of open-circuit photovoltage with long alkyl group. *Chemistry of Materials* **2011**, *23*, 4394-4401, https://doi.org/10.1021/cm202226j.
30. Yum, J.H.; Holcombe, T.W.; Kim, Y.; Yoon, J.; Rakstys, K.; Nazeeruddin, M.K.; Grätzel, M. Towards high-performance DPP-based sensitizers for DSC applications. *Chemical Communications* **2012**, *48*, 10727-10729, https://doi.org/10.1039/c2cc35597c.
31. Zhu, H.; Li, W.; Wu, Y.; Liu, B.; Zhu, S.; Li, X.; Ågren, H.; Zhu, W. Insight into benzothiadiazole acceptor in D-A-π-A configuration on photovoltaic performances of dye-sensitized solar cells. *ACS Sustainable Chemistry and Engineering* **2014**, *2*, 1026-1034, https://doi.org/10.1021/sc500035j.
32. Zhu, W.; Wu, Y.; Wang, S.; Li, W.; Li, X.; Chen, J.; Wang, Z.S.; Tian, H. Organic D-A-π-A solar cell sensitizers with improved stability and spectral response. *Advanced Functional Materials* **2011**, *21*, 756-763, https://doi.org/10.1002/adfm.201001801.

33. Zhang, H.; Iqbal, Z.; Chen, Z.-E.; Hong, Y. Synthesis of Novel Sensitizers with a Linear Conjugated Di(1-benzothieno)[3,2-b:2',3'-d]pyrrole Unit for Dye-Sensitized Solar Cells. *Dyes and Pigments* **2018**, *162*, 89-96, https://doi.org/10.1016/j.dyepig.2018.10.004.
34. Al-Ghamdi, S.N.; Al-Ghamdi, H.A.; El-Shishtawy, R.M.; Asiri, A.M. Advances in phenothiazine and phenoxazine-based electron donors for organic dye-sensitized solar cells. *Dyes and Pigments* **2021**, *194*, https://doi.org/10.1016/j.dyepig.2021.109638.
35. Mahmood, A. Triphenylamine based dyes for dye sensitized solar cells: A review. *Solar Energy* **2016**, *123*, 127-144, https://doi.org/10.1016/j.solener.2015.11.015.
36. Jung, C.Y.; Song, C.J.; Yao, W.; Park, J.M.; Hyun, I.H.; Seong, D.H.; Jaung, J.Y. Synthesis and performance of new quinoxaline-based dyes for dye sensitized solar cell. *Dyes and Pigments* **2015**, *121*, 204-210, https://doi.org/10.1016/j.dyepig.2015.05.019.
37. Pounraj, P.; Mohankumar, V.; Pandian, M.S.; Ramasamy, P. The effect of different π-bridge configuration on bi-anchored triphenylamine and phenyl modified triphenylamine based dyes for dye sensitized solar cell (DSSC) application: A theoretical approach. *Journal of Molecular Graphics and Modelling* **2018**, *79*, 235-253, https://doi.org/10.1016/j.jmgm.2017.12.004.
38. Becke, A.D. Density-fnnctional exchange-energy approximation with correct asymptotic behavior. *Physical Review A* **1988**, *38*, 3098-3100.
39. Krishnan, R.; Binkley, J.S.; Seeger, R.; Pople, J.A. Self-consistent molecular orbital methods. XX. A basis set for correlated wave functions. *The Journal of Chemical Physics* **1980**, *72*, 650-654, https://doi.org/10.1063/1.438955.
40. Frisch, M.; Trucks, G.W.; Schlegel, H.B.; Scuseria, G.E.; Robb, M.A.; Cheeseman, J.R.; Scalmani, G.; Barone, V.; Mennucci, B.; Petersson, G. Gaussian 09, Rev. A.02. **2009**.
41. Gross, E.K.U.; Kohn, W. *Time Dependent Density Functional Theory*. **1990**; pp. 254-259.
42. Yanai, T.; Tew, D.P.; Handy, N.C. A new hybrid exchange–correlation functional using the Coulomb-attenuating method (CAM-B3LYP). *Chemical physics letters* **2004**, *393*, 51-57, https://doi.org/10.1016/j.cplett.2004.06.011.
43. Preat, J.; Michaux, C.; Jacquemin, D.; Perpète, E.A. Enhanced efficiency of organic dye-sensitized solar cells: Triphenylamine derivatives. *Journal of Physical Chemistry C* **2009**, *113*, 16821-16833, https://doi.org/10.1021/jp904946a.
44. Chen, X.K.; Zou, L.Y.; Ren, A.M.; Fan, J.X. How dual bridging atoms tune structural and optoelectronic properties of ladder-type heterotetracenes? - A theoretical study. *Physical Chemistry Chemical Physics* **2011**, *13*, 19490-19498, https://doi.org/10.1039/c1cp22227a.
45. Hagfeldt, A.; Graetzel, M. Light-Induced Redox Reactions in Nanocrystalline Systems. *Chemical Reviews* **1995**, *95*, 49-68, https://doi.org/10.1021/cr00033a003.
46. Singh, P.; Ravindra, N.M. Temperature dependence of solar cell performance - An analysis. *Solar Energy Materials and Solar Cells* **2012**, *101*, 36-45, https://doi.org/10.1016/j.solmat.2012.02.019.
47. Xu, J.; Zhu, L.; Fang, D.; Chen, B.; Liu, L.; Wang, L.; Xu, W. Substituent effect on the π linkers in triphenylamine dyes for sensitized solar cells: A DFT/TDDFT study. *ChemPhysChem* **2012**, *13*, 3320-3329, https://doi.org/10.1002/cphc.201200273.
48. Zhang, J.; Li, H.B.; Sun, S.L.; Geng, Y.; Wu, Y.; Su, Z.M. Density functional theory characterization and design of high-performance diarylamine-fluorene dyes with different π spacers for dye-sensitized solar cells. *Journal of Materials Chemistry* **2012**, *22*, 568-576, https://doi.org/10.1039/c1jm13028e.
49. Asbury, J.B.; Wang, Y.-Q.; Hao, E.; Ghosh, H.N.; Lian, T. Evidences of hot excited state electron injection from sensitizer molecules to TiO 2 nanocrystalline thin films. *Research on Chemical Intermediates* **2001**, *27*, 393-406, https://doi.org/10.1163/156856701104202255.
50. Hinkel, F.; Kim, Y.M.; Zagraniarsky, Y.; Schlütter, F.; Andrienko, D.; Müllen, K.; Laquai, F. Efficiency-limiting processes in cyclopentadithiophene-bridged donor-acceptor-type dyes for solid-state dye-sensitized solar cells. *Journal of Chemical Physics* **2018**, *148*, 044703-044708, https://doi.org/10.1063/1.4999136.
51. Pounraj, P.; Mohankumar, V.; Pandian, M.S.; Ramasamy, P. Donor functionalized quinoline based organic sensitizers for dye sensitized solar cell (DSSC) applications: DFT and TD-DFT investigations. *Journal of Molecular Modeling* **2018**, *24*, https://doi.org/10.1007/s00894-018-3872-8.
52. Bai, Y.; Zhang, J.; Zhou, D.; Wang, Y.; Zhang, M.; Wang, P. Engineering organic sensitizers for iodine-free dye-sensitized solar cells: Red-shifted current response concomitant with attenuated charge recombination. *Journal of the American Chemical Society* **2011**, *133*, 11442-11445, https://doi.org/10.1021/ja203708k.
53. Raftani, M.; Abram, T.; Kacimi, R.; Bennani, M.N.; Bouachrine, M. Organic compounds based on pyrrole and terphenyl for organic light-emitting diodes (OLED) applications : Design and electro-optical properties. *J. Mater. Environ. Sci.* **2020**, *11*, 933-946.
54. Hutchison, G.R.; Ratner, M.A.; Marks, T.J. Hopping transport in conductive heterocyclic oligomers: Reorganization energies and substituent effects. *Journal of the American Chemical Society* **2005**, *127*, 2339-2350, https://doi.org/10.1021/ja0461421.
55. Liu, S. Dynamic behavior of chemical reactivity indices in density functional theory: A Bohn-Oppenheimer quantum molecular dynamics study. *Journal of Chemical Sciences* **2005**, *117*, 477-483, https://doi.org/10.1007/BF02708352.

56. Parr, R.G.; Donnelly, R.A.; Levy, M.; Palke, W.E. Electronegativity: The density functional viewpoint. *The Journal of Chemical Physics* **2003**, *68*, 3801-3807, https://doi.org/10.1063/1.436185.
57. Pearson, R.G. Hard and Soft Acids and Bases. *Journal of the American Chemical Society* **1963**, *85*, 3533-3539, https://doi.org/10.1021/ja00905a001.
58. Parr, R.G.; Pearson, R.G. Absolute Hardness: Companion Parameter to Absolute Electronegativity. *Journal of the American Chemical Society* **1983**, *105*, 7512-7516, https://doi.org/10.1021/ja00364a005.
59. Bedda, T.; Benharref, A.; Elabdellaoui, H.E. Theoretical Study By D.F.T. Of Region And Stereo-Selectivity Of Condensation Of β-Himachalene With m-Chloroperbenzoic Acid (m-CPBA) In Dichloromethane. *International Journal of Innovation and Applied Studies* **2014**, *8*, 720-727.
60. Chattaraj, P.K.; Maiti, B. HSAB principle applied to the time evolution of chemical reactions. *Journal of the American Chemical Society* **2003**, *125*, 2705-2710, https://doi.org/10.1021/ja0276063.
61. El Assyry, A.; Jdaa, R.; Benali, B.; Addou, M.; Zarrouk, A. Optical and photovoltaic properties of new quinoxalin-2(1H)-one-based D-A organic dyes for efficient dye-sensitized solar cell using DFT. *Journal of Materials and Environmental Science* **2015**, *6*, 2612-2623.
62. Azaid, A.; Abram, T.; Kacimi, R.; Sbai, A.; lakhlifi, T.; Bouachrine, M. Organic materials based with D– π –A structure based on thiophene and anthracene for application in dye-sensitized solar cells. *Materials Today: Proceedings* **2021**, *45*, 7363-7369, https://doi.org/10.1016/j.matpr.2021.01.119.
63. Li, M.; Kou, L.; Diao, L.; Zhang, Q.; Li, Z.; Wu, Q.; Lu, W.; Pan, D. Theoretical study of Acene-bridged dyes for dye-sensitized solar cells. *Journal of Physical Chemistry A* **2015**, *119*, 3299-3309, https://doi.org/10.1021/acs.jpca.5b00798.
64. Vuai, S.A.H.; Khalfan, M.S.; Babu, N.S. DFT and TD-DFT studies for optoelectronic properties of coumarin based donor-π-acceptor (D-π-A) dyes: applications in dye-sensitized solar cells (DSSCS). *Heliyon* **2021**, *7*, https://doi.org/10.1016/j.heliyon.2021.e08339.
65. Bourass, M.; Benjelloun, A.; Benzakour, M.; McHarfi, M.; Hamidi, M.; Bouzzine, S.M.; Serein-Spirau, F.; Jarrosson, T.; Lère-Porte, J.; Sotiropoulos, J.-M.; Bouachrine, M.; Meknes; Morocco. The Computational Study Of The electronic and Optoelectronics Properties of New Materials Based On Thienopyrazine For Application in Dye Solar Cells. *Journal of Materials and Environmental Science* **2016**, *7*, 700-712.
66. Kacimi, R.; Bourass, M.; Toupance, T.; Wazzan, N.; Chemek, M.; El Alamy, A.; Bejjit, L.; Alimi, K.; Bouachrine, M. Computational design of new organic (D–π–A) dyes based on benzothiadiazole for photovoltaic applications, especially dye-sensitized solar cells. *Research on Chemical Intermediates* **2020**, *46*, 3247-3262, https://doi.org/10.1007/s11164-020-04150-7.
67. Keller, N.; Bein, T. Optoelectronic processes in covalent organic frameworks. *Chem Soc Rev* **2021**, *50*, 1813-1845, https://doi.org/10.1039/d0cs00793e.
68. Fitri, A.; Benjelloun, A.T.; Benzakour, M.; McHarfi, M.; Hamidi, M.; Bouachrine, M. Theoretical investigation of new thiazolothiazole-based D-π-A organic dyes for efficient dye-sensitized solar cell. *Spectrochimica Acta - Part A: Molecular and Biomolecular Spectroscopy* **2014**, *124*, 646-654, https://doi.org/10.1016/j.saa.2014.01.052.
69. Raftani, M.; Abram, T.; Loued, W.; Azaid, A.; Kacimi, R.; Alimi, K.; Bennani, M.N.; Bouachrine, M. The optoelectronic properties of π-conjugated organic molecules based on terphenyl and pyrrole for BHJ solar cells: DFT / TD-DFT theoretical study. *Current Chemistry Letters* **2021**, *10*, 1-14, https://doi.org/10.5267/j.ccl.2021.4.002.
70. Raftani, M.; Abram, T.; Bennani, M.N.; Bouachrine, M. Theoretical Study Of New Conjugated Compounds With A Low Bandgap For Bulk Heterojunction Solar Cells: DFT And TD-DFT Study. *Results in Chemistry* **2020**, *2*, 138277-138277, https://doi.org/10.1016/j.rechem.2020.100040.
71. Joseph, V.; Thomas, K.R.J.; Sahoo, S.; Singh, M.; Jou, J.-H. Asymmetrically 2,7-difunctionalized carbazole-based donor-acceptor hybrids for deep blue electroluminescence applications. *Optical Materials* **2020**, *108*, https://doi.org/10.1016/j.optmat.2020.110159.
72. Kacimi, R.; Raftani, M.; Abram, T.; Azaid, A.; Ziyat, H.; Bejjit, L.; Bennani, M.N.; Bouachrine, M. Theoretical design of D-pi-A system new dyes candidate for DSSC application. *Heliyon* **2021**, *7*, https://doi.org/10.1016/j.heliyon.2021.e07171.
73. T.Abram; R.Kacimi; L.Bejjit; M.Bouachrine. New Molecules Based On Thiophene and Oxathiazole for Solar, Organic Application, Cells. *RHAZES: Green and Applied Chemistry* **2018**, *1*, 31-37.
74. Semire, B.; Oyebamiji, A.K.; Odunola, O.A. Electronic properties' modulation of D–A–A via fluorination of 2-cyano-2-pyran-4-ylidene-acetic acid acceptor unit for efficient DSSCs: DFT-TDDFT approach. *Scientific African* **2020**, *7*, e00287-e00287, https://doi.org/10.1016/j.sciaf.2020.e00287.
75. Liang, J.; Tang, X.; Yin, P.; Weng, C.; Shen, P. Development of new nonacyclic small-molecule acceptors involving two benzo[1,2-b:4,5-b′]dithiophene moieties for efficient polymer solar cells. *Synthetic Metals* **2021**, *282*, https://doi.org/10.1016/j.synthmet.2021.116922.
76. Pearson, R.G. *Chemical Hardness: Applications from Molecules to Solids*. 1st Edition ed.; Wiley-VCH: **1997**; pp. 208-208.
77. Benabid, S.; Streit, A.F.M.; Benguerba, Y.; Dotto, G.L.; Erto, A.; Ernst, B. Molecular modeling of anionic and cationic dyes adsorption on sludge derived activated carbon. *Journal of Molecular Liquids* **2019**, *289*, 111119-111119, https://doi.org/10.1016/j.molliq.2019.111119.

78. Abusaif, M.S.; Fathy, M.; Abu-Saied, M.A.; Elhenawy, A.A.; Kashyout, A.B.; Selim, M.R.; Ammar, Y.A. New carbazole-based organic dyes with different acceptors for dye-sensitized solar cells: Synthesis, characterization, dssc fabrications and density functional theory studies. *Journal of Molecular Structure* **2021**, *1225*, https://doi.org/10.1016/j.molstruc.2020.129297.
79. Shakila, G.; Saleem, H.; Sundaraganesan, N. FT-IR , FT-Raman , NMR and U-V Spectral investigation : Computation of vibrational frequency , chemical shifts and electronic structure calculations of 1-bromo-4-nitrobenzene. *World Scientific News* **2017**, *61*, 150-185.
80. Sen, J.S.M.K. *Molecular Electrostatic Potentials: Concepts and Applications*, 1 ed.; Elsevier Science; 1 edition (November 22, 1996): **1996;** pp. 664.
81. Bouzayen, N.; Mbarek, M.; Alimi, K. Solvent effects on optical and electronic properties of carbazole benzothiazole based bipolar compound: TD-DFT / PCM approach. *Computational and Theoretical Chemistry* **2015**, *3*, 28-39, https://doi.org/10.48317/IMIST.PRSM/morjchem-v3i1.2259.
82. Prabavathi, N.; Nilufer, A.; Krishnakumar, V. Vibrational spectroscopic (FT-iR and FT-Raman) studies, natural bon orbital analysis and molecular electrostatic potential surface of isoxanthopterin. *Molecular and Biomolecular Spectroscopy* **2013**, *114*, 101-113, https://doi.org/10.1016/j.saa.2013.05.013.
83. Qu, S.; Wu, W.; Hua, J.; Kong, C.; Long, Y.; Tian, H. New diketopyrrolopyrrole (DPP) dyes for efficient dye-sensitized solar cells. *Journal of Physical Chemistry C* **2010**, *114*, 1343-1349, https://doi.org/10.1021/jp909786k.
84. Zhang, C.R.; Liu, L.; Zhe, J.W.; Jin, N.Z.; Ma, Y.; Yuan, L.H.; Zhang, M.L.; Wu, Y.Z.; Liu, Z.J.; Chen, H.S. The role of the conjugate bridge in electronic structures and related properties of tetrahydroquinoline for dye sensitized solar cells. *International Journal of Molecular Sciences* **2013**, *14*, 5461-5481, https://doi.org/10.3390/ijms14035461.
85. Abdullah, M.I.; Janjua, M.R.S.A.; Mahmood, A.; Ali, S.; Ali, M. Quantum chemical designing of efficient sensitizers for dye sensitized solar cells. *Bulletin of the Korean Chemical Society* **2013**, *34*, 2093-2098, https://doi.org/10.5012/bkcs.2013.34.7.2093.
86. Luo, J.H.; Li, Q.S.; Yang, L.N.; Sun, Z.Z.; Li, Z.S. Theoretical design of porphyrazine derivatives as promising sensitizers for dye-sensitized solar cells. *RSC Advances* **2014**, *4*, 20200-20207, https://doi.org/10.1039/c4ra02204a.
87. Roy, J.K.; Kar, S.; Leszczynski, J. Insight into the optoelectronic properties of designed solar cells efficient tetrahydroquinoline dye-sensitizers on TiO2(101) surface: first principles approach. *Scientific Reports* **2018**, *8*, 1-12, https://doi.org/10.1038/s41598-018-29368-9.
88. Yang, L.; Feng, J.K.; Ren, A.M. Theoretical studies on the electronic and optical properties of two thiophene-fluorene based π-conjugated copolymers. *Polymer* **2005**, *46*, 10970-10981, https://doi.org/10.1016/j.polymer.2005.09.050.
89. Zou, L.Y.; Ren, A.M.; Feng, J.K.; Ran, X.Q. Theoretical design study on multifunctional triphenyl amino-based derivatives for OLEDs. *Journal of Physical Organic Chemistry* **2009**, *22*, 1104-1113, https://doi.org/10.1002/poc.1565.
90. Ait Aicha, Y.; Bouzzine, S.M.; Fahim, Z.M.; Zair, T.; Bouachrine, M.; Hamidi, M. Quantum chemical investigations study of the effect of electron donor units on the structural, electronic and optoelectronic properties of diarylthienopyrazine analogs. *Computational and Theoretical Chemistry* **2014**, *1036*, 22-30, https://doi.org/10.1016/j.comptc.2014.03.008.
91. Erdogdu, Y.; Baskose, U.C.; Saglam, S.; Erdogdu, M.; Ogutcu, H.; Özçelik, S. Structural, thermal, spectroscopic, electronic and biological activity properties of coumarin-153 dyes for DSSCs: A DFT benchmark study. *Journal of Molecular Structure* **2020**, *1221*, https://doi.org/10.1016/j.molstruc.2020.128873.
92. Nitschke, P.; Jarzabek, B.; Damaceanu, M.D.; Bejan, A.E.; Chaber, P. Spectroscopic and electrochemical properties of thiophene-phenylene based Shiff-bases with alkoxy side groups, towards photovoltaic applications. *Spectrochim Acta A Mol Biomol Spectrosc* **2021**, *248*, https://doi.org/10.1016/j.saa.2020.119242.